Scientific
Research

The Structure of Modified Fe-Ni Bioxide Composite Nanoparticles Using Fe(NO$_3$)$_3$

Yueqiang Lin[1], Jian Li[1*], Lihua Lin[1], Xiaodong Liu[1], Longlong Chen[1], Decai Li[2]

[1]School of Physical Science & Technology, Southwest University, Chongqing, China
[2]School of Mechanical and Control Engineering, Beijing Jiaotong University, Beijing, China
Email: [*]aizhong@swu.edu.cn

ABSTRACT

Composite nanoparticles containing a γ-Fe$_2$O$_3$ core, Ni$_2$O$_3$ external shell and FeCl$_3 \cdot$6H$_2$O outermost layer can be synthesized by chemically induced transition in FeCl$_2$ solution. These may be modified by treatment with Fe(NO$_3$)$_3$ to obtain particles for the preparation of ionic ferrofluids. Vibrating sample magnetometer (VSM) measurements and transmission electron microscopy (TEM) observations show that after Fe(NO$_3$)$_3$ treatment, the specific magnetization becomes weaker and the size becomes larger for treated particles compared with the untreated particles. Using energy dispersive X-ray spectroscopy (EDX), X-ray diffraction (XRD) and X-ray photoelectron spectroscopy (XPS), the structure of the particles before and after the treatment is revealed. The experimental results show that the γ-Fe$_2$O$_3$ core is unchanged, the Ni$_2$O$_3$ is dissolved partially and the FeCl$_3 \cdot$6H$_2$O is replaced by Fe(NO$_3$)$_3 \cdot$9H$_2$O. The percentages of molar, mass and volume of these phases are deduced, and the average density of the modified particles is also estimated.

1. Introduction

Magnetic nanoparticles are an important class of nanoscopic magnetic systems. The preparation and characterization of magnetic nanoparticles have attracted increasing interest as particles in this size range may allow investigation of fundamental aspects of magnetic-ordering phenomena in magnetic materials with reduced dimension and could lead to new technological applications [1,2]. A nanocomposite is a material composed of two or more phases in which the combination of different physical or chemical properties may lead to completely novel materials [3]. In addition, magnetic nanocomposites have applications that range from ferrofluids to separation science and technology [4].

Ferrofluids (magnetic fluids) can be synthesized by dispersing nanosized subdomain magnetic particles of ~10 nm in diameter in a carrier liquid. Generally, magnetic nanoparticles in ferrofluids are coated with a surfactant to prevent aggregation [5]. In the 1980s, Massart proposed a method for chemical synthesis of ferrofluids with no surfactant [6]. This method has subsequently been called the Massart's method and such ferrofluids are known as ionic ferrofluids or electrical double-layered ferrofluids [7,8]. In an adaptation of Massart's method for the synthesis of the ferrofluids, magnetic nanoparticles need to be treated with ferric nitrate to yield a chemically stable particle surface.

Magnetization (moment per unit volume) M is an important physical parameter used to characterize magnetic materials. In practice, the volume of a particle Vp is too difficult to measure directly, so the magnetization is obtained usually from M = $\sigma \cdot \rho$, where σ is the specific magnetization (moment per unit mass) and ρ is the known density of the constituent materials [9]. In addition, the volume fraction of particles in ferrofluids, ϕ_v = Vp/(Vp + Vc), where Vp is the volume of the particles and Vc is the volume of the carrier liquid, is also an important characteristic parameter to which the behavior of ferrofluids is related [10]. Therefore, volume of the particles is an important feature for magnetic nanoparticles and is generally obtained from an accurate measure of the mass m and the known density ρ, *i.e.* Vp = m/ρ. However, if the nanoparticles consist of different chemical compounds, the density of the particles is no longer

---
[*]Corresponding author.

uniform, and their volume cannot be determined by measuring just their mass.

Recently, we have proposed a method to prepare Fe-Ni bioxide composite nanoparticles by a chemically induced transition [11]. These nanoparticles might be very suitable for the synthesis of ionic ferrofluids [12]. In the present work, untreated Fe-Ni bioxide composite nanoparticles and those treated with ferric nitrate have been characterized, and their chemical compositions and average density were studied.

2. Experimental

The γ-Fe_2O_3/Ni_2O_3 composite nanoparticles were prepared by the so-called chemically induced transition method. The preparation can be divided into two steps. Firstly, an aqueous mixture of $FeCl_3$ (40 ml, 1 M) and $Ni(NO_3)_3$ (10 ml, 2 M; in HCl 0.05 ml) was added to NaOH solution (500 ml, 0.7 M). Then the solution was heated and boiled for 5 min, after which the black precursor gradually precipitated. Secondly, the precursor was added to $FeCl_2$ solution (400 ml, 0.25 M), which was then heated to boiling point for 30 min. The nanoparticles were again precipitated after the heating had stopped. After washing to pH = 7 with very dilute aqueous HNO_3 solution ($\leq$0.01 M), the as-prepared particles (the untreated particles) were added to boiling $Fe(NO_3)_3$ solution (400 ml, 0.25 M), which was then kept boiling for 30 min. The particles were then dehydrated with acetone and allowed to dry naturally to yield the modified particles (the treated particles).

The magnetization, morphology, bulk chemical species, crystal structure and surface chemical compositions of the particles were investigated using a vibrating sample magnetometer (VSM, HH-15), transmission electron microscopy (TEM, TecnaiG220), energy dispersive X-ray spectroscopy (EDX, Quanta-200), X-ray diffraction (XRD, XD-12) and X-ray photoelectron spectroscopy (XPS, SAM800). The phase structures of the particles were determined from the experimental results.

3. Results and Analysis

The specific magnetization curves are shown in **Figure 1**. Clearly, the magnetization of the treated particles is weaker than that of the untreated particles. From the plots of σ vs. 1/H in high field [13] the specific saturation magnetizations σ_s are evaluated as 56.59 emu/g and 41.19 emu/g for the untreated and treated particles, respectively.

TEM observations show that both untreated and treated particles were spherical. **Figure 2** is a typical TEM micrograph of the particles. Statistical analysis reveals that the size of the particles fits a log-normal distribution. For the untreated particles, the median diameter
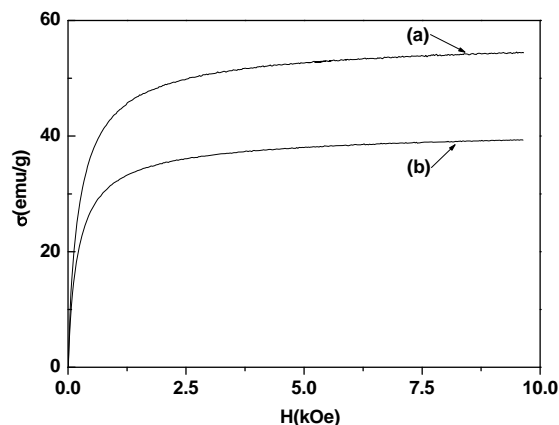
Figure 1. The specific magnetization curves of (a) untreated particles and (b) treated particles.
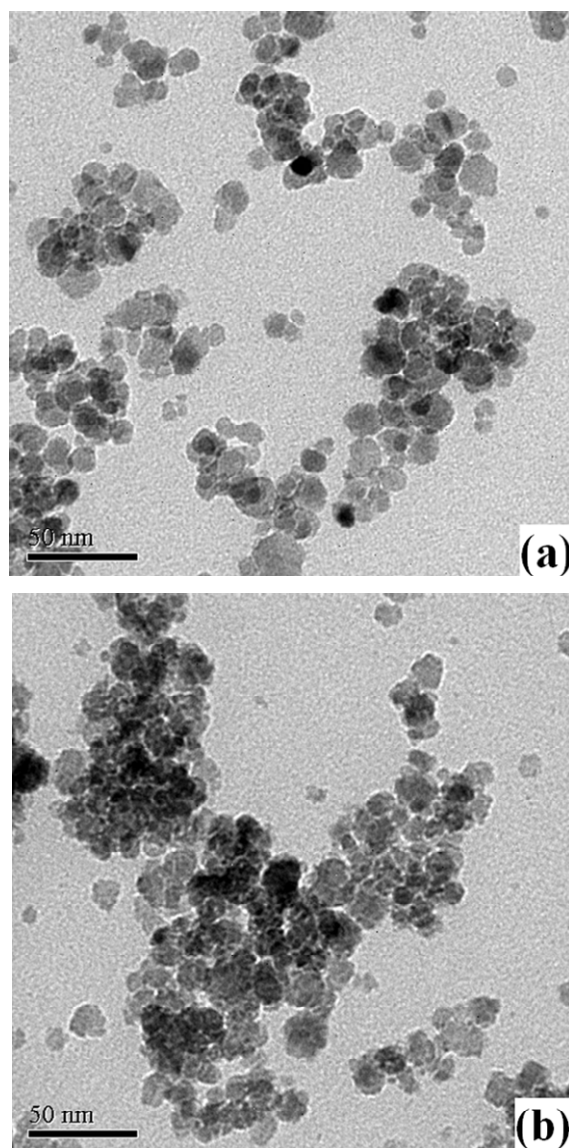
Figure 2. Typical TEM images of (a) untreated particles and (b) treated particles.

dg is 10.78 nm and the standard deviation $\ln\sigma_g$ is 0.27; for the treated particles, dg is 11.43 nm and $\ln\sigma_g$ is 0.26. The average diameter $<d>$ is calculated from $<d> = \exp[\ln dg + 0.5\ln^2\sigma_g]$ [14] and gives.11.18 nm for the untreated particles, and 11.82 nm for the treated particles.

The results of the EDX measurements indicated that both untreated and treated particles had O, Fe and Ni species, but the untreated particles also contained Cl and the treated particles contained N and Cl. The atomic percentages a_i for these elements are listed in **Table 1**.

Figure 3 shows the XRD patterns for the two nanoparticles. For the untreated particles, the major diffraction peaks corresponded to γ-Fe_2O_3 (magnetite, PDF# 39-1346), with some weaker peaks corresponding to Ni_2O_3 (PDF#14-0481). No clear diffraction peaks corresponded to any phase based on the Cl species. In addition, for the treated particles, diffraction peaks were present for both γ-Fe_2O_3 and Ni_2O_3. However, by comparing with the pattern of untreated particles, it was found that the diffraction intensity of Ni_2O_3 had been weakened relative to that of γ-Fe_2O_3. In addition, some new diffraction peaks appeared, as indicated by arrows A, B, C and D. These are close to the d=0.2620, 0.2550, 0.1900 and 0.1700 nm peaks of $Fe(NO_3)_3\cdot 9H_2O$ (PDF#01-0124).
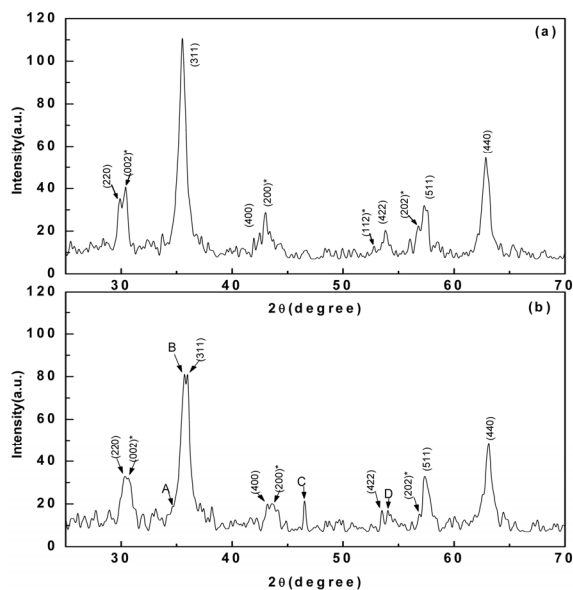
Figure 3. XRD patterns of (a) untreated particles and (b) treated particles. The peaks (h k l) correspond to γ-Fe_2O_3 (PDF#39-1346) and peaks (h k l)* correspond to Ni_2O_3 (PDF#14-0481).

Table 1. The atomic composition from EDX measurement a_i.

i	O	Fe	Ni	Cl	N
Untreated particles	56.82	39.15	2.37	1.66	
Treated particles	60.33	35.60	1.57		2.50

The XPS spectra are shown in **Figure 4**. These confirm the presence of the same chemical species as determined by the EDX measurements. Combining the EDX and XRD results, it was apparent that besides γ-Fe_2O_3 and Ni_2O_3, there was also a phase based on Cl in the untreated particles and $Fe(NO_3)_3\cdot 9H_2O$ was present in the treated particles. As a result, the O1s and Fe2p3/2 lines are split, as shown in **Figure 5**. The detailed binding energy data are listed in **Table 2**. To summarize, these measurements precisely identify γ-Fe_2O_3, Ni_2O_3 and $FeCl_3$ phases in the untreated particles and γ-Fe_2O_3, Ni_2O_3 and $Fe(NO_3)_3\cdot 9H_2O$ phases in treated particles. In the untreated particles, the $FeCl_3$ phase could contain
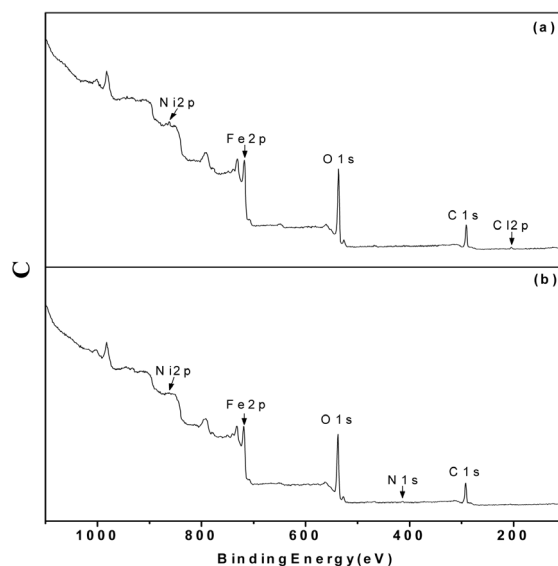
Figure 4. XPS spectra of (a) untreated particles and (b) treated particles.

Table 2. The binding energy data from XPS measurements (eV).

	O_1s		$Fe_2p_{3/2}$		$Ni_2p_{3/2}$	Cl_2p
Untreated particles	529.8P1	531.8P2	710.2P1	711.0P2	854.9	198.1
γ-Fe_2O_3	529.8		710.9			
Ni_2O_3		531.8			855.6	
$FeCl_3$				711.0		198.0

	O_1s			$Fe_2p_{3/2}$		$Ni_2p_{3/2}$	N_1s
Treated particles	529.8 P1	531.1P2	532.3P3	710.4P1	711.3P2	854.8	406.3
γ-Fe_2O_3	529.8			710.9			
Ni_2O_3		531.8				855.6	
$Fe(NO_3)_3$			532.93	710.09			406.7

Note: The standard data for γ-Fe_2O_3, Ni_2O_3, $FeCl_3$ are taken from the Handbook of X-ray photoelectron spectroscopy. Data for $Fe(NO_3)_3\cdot 9H_2O$ are taken from Ref. [16].
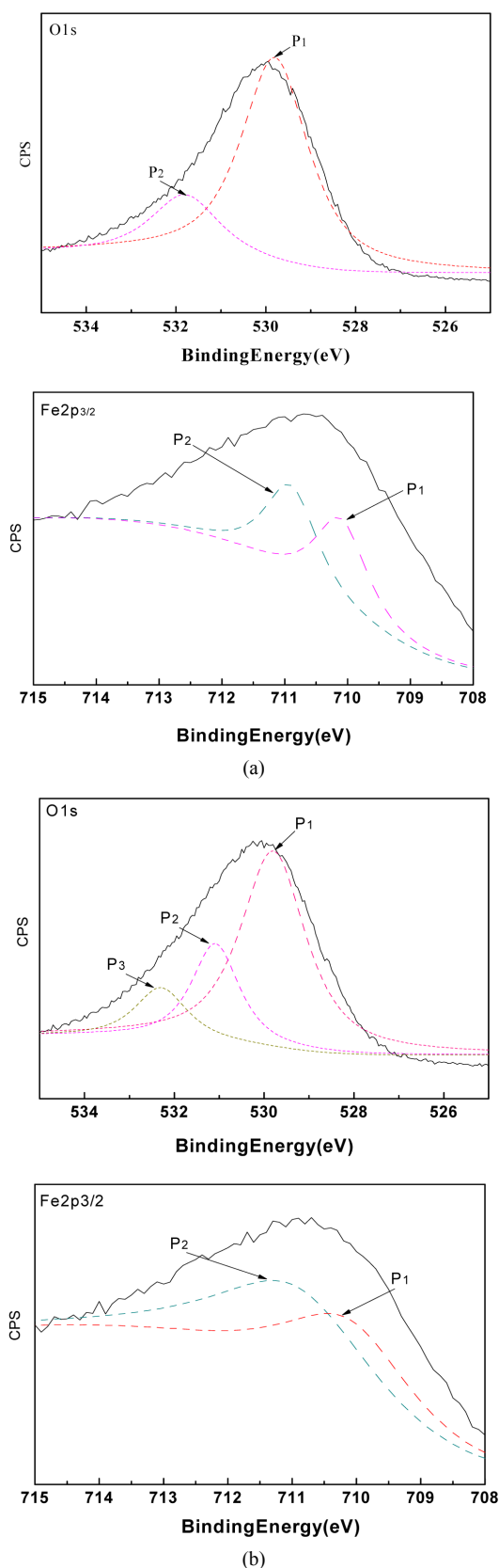
Figure 5. XPS results of O$_1$s lines and Fe Fe$_2$p$_{3/2}$ lines for (a) untreated particles and (b) treated particles.

water of crystallization, as in FeCl$_3$·6·H$_2$O, since this compound is formed on the γ-Fe$_2$O$_3$ cores, when these are synthesized by a similar, chemically induced transition method in FeCl$_2$ solution [15].

4. Discussion

4.1. The Structure of the Particles

The experimental results and analysis above reveal that both untreated and treated particles are spherical nano-particles with sizes of the order of 10 nm. The untreated particles consist of γ-Fe$_2$O$_3$, Ni$_2$O$_3$ and FeCl$_3$·6H$_2$O phases. There must be very little FeCl$_3$·6H$_2$O since there were no clear corresponding diffraction peaks in the XRD pattern. In addition, in the treated particles, Fe(NO$_3$)$_3$·9H$_2$O is present as well as the γ-Fe$_2$O$_3$ and Ni$_2$O$_3$ phases, but no FeCl$_3$·6H$_2$O. Comparing with the untreated particles, the proportion of Ni$_2$O$_3$ is lower in the treated particles. We conclude that during the treatment, FeCl$_3$·6H$_2$O and some Ni$_2$O$_3$ are dissolved and Fe(NO$_3$)$_3$·9H$_2$O is formed instead. As a consequence, it appears that the untreated nanoparticles consist of a γ-Fe$_2$O$_3$ core, Ni$_2$O$_3$ external shell and FeCl$_3$·6H$_2$O outermost layer; the treated particles have the same core and external shell, but Fe(NO$_3$)$_3$·9H$_2$O outermost layer. A schematic structural diagram of the particles is presented in **Figure 6**. It appears that the γ-Fe$_2$O$_3$ core remains unchanged when the particles are treated in Fe(NO$_3$)$_3$ solution.

4.2. The Molar Percentages of the Phases in the Particles

The structural data and the quantitative elemental analysis from the EDX measurements provide a description of the molar ratios of the phases for both particles, as follows.

For the untreated particles, based on γ-Fe$_2$O$_3$, Ni$_2$O$_3$ and FeCl$_3$·6H$_2$O phases, the molar ratio between the γ-Fe$_2$O$_3$ and Ni$_2$O$_3$ phases, $y_{\gamma/Ni}$, can be written as

$$y_{\gamma/Ni} = \frac{y_\gamma \left(\gamma - Fe_2O_3 \left(mol\right)\right)}{y_{Ni} \left(Ni_2O_3 \left(mol\right)\right)} \frac{a_{Cl}}{a_{Ni}} \left(\frac{a_{Fe}}{a_{Cl}} - \frac{1}{3}\right) \quad (1)$$

where a_{Fe}, a_{Ni} and a_{Cl} are the atomic percentages of Fe, Ni and Cl, respectively. Likewise, the ratio between the
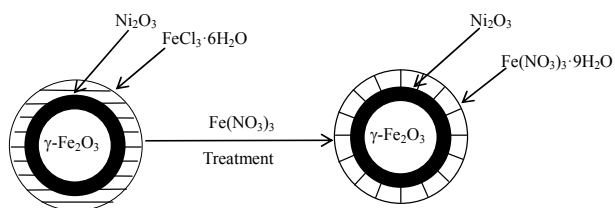
Figure 6. Schematic model of the structures of the particles.

γ-Fe$_2$O$_3$ and FeCl$_3$ phases, $y_{\gamma/\text{Cl}}$, can be written as

$$y_{\gamma/\text{Cl}} = \frac{y_\gamma \left(\gamma - \text{Fe}_2\text{O}_3 \left(\text{mol}\right)\right)}{y_{\text{Cl}} \left(\text{FeCl}_3 \left(\text{mol}\right)\right)} = \frac{3}{2}\left(\frac{a_{\text{Fe}}}{a_{\text{Cl}}} - \frac{1}{3}\right) \quad (2)$$

Consequently, the molar percentages of γ-Fe$_2$O$_3$ $\left(y_\gamma\right)$, Ni$_2$O$_3$ $\left(y_{\text{Ni}}\right)$ and FeCl$_3$ $\left(y_{\text{Cl}}\right)$ can be obtained as

$$y_\gamma = \frac{1}{1 + \dfrac{1}{y_{\gamma/\text{Ni}}} + \dfrac{1}{y_{\gamma/\text{Cl}}}} \times 100, \; y_{\text{Ni}} = \frac{y_\gamma}{y_{\gamma/\text{Ni}}}, \; y_{\text{Cl}} = \frac{y_\gamma}{y_{\gamma/\text{Cl}}} \quad (3)$$

From the EDX data listed in **Table 1**, the values of y_γ, y_{Ni} and y_{Cl} can be calculated and these are given in **Table 3**.

For the treated particles based on γ-Fe$_2$O$_3$, Ni$_2$O$_3$ and Fe(NO$_3$)$_3$·9H$_2$O phases, $y_{\gamma/\text{Ni}}$, can be written as

$$y_{\gamma/\text{Ni}} = \frac{y_\gamma \left(\gamma - \text{Fe}_2\text{O}_3 \left(\text{mol}\right)\right)}{y_{\text{Ni}} \left(\text{Ni}_2\text{O}_3 \left(\text{mol}\right)\right)} = \frac{a_{\text{N}}}{a_{\text{Ni}}}\left(\frac{a_{\text{Fe}}}{a_{\text{N}}} - \frac{1}{3}\right) \quad (4)$$

where a_{Fe}, a_{Ni} and a_{N} are the atomic percentages of Fe, Ni and N, respectively. Likewise, the ratio between γ-Fe$_2$O$_3$ and Fe(NO$_3$)$_3$ phases, $y_{\gamma/\text{N}}$, can be written as

$$y_{\gamma/\text{N}} = \frac{y_\gamma \left(\gamma - \text{Fe}_2\text{O}_3 \left(\text{mol}\right)\right)}{y_{\text{N}} \left(\text{FeCl}_3 \left(\text{mol}\right)\right)} = \frac{3}{2}\left(\frac{a_{\text{Fe}}}{a_{\text{N}}} - \frac{1}{3}\right) \quad (5)$$

Thus, the molar percentages of γ-Fe$_2$O$_3$ $\left(y_\gamma\right)$, Ni$_2$O$_3$ $\left(y_{\text{Ni}}\right)$ and Fe(NO$_3$)$_3$ $\left(y_{\text{N}}\right)$ for the treated particles, can be obtained from

$$y_\gamma = \frac{1}{1 + \dfrac{1}{y_{\gamma/\text{Ni}}} + \dfrac{1}{y_{\gamma/\text{N}}}} \times 100, \; y_{\text{Ni}} = \frac{y_\gamma}{y_{\gamma/\text{Ni}}}, \; y_{\text{N}} = \frac{y_\gamma}{y_{y_{\gamma/\text{N}}}} \quad (6)$$

The values of y_γ, y_{Ni} and y_{N} can be calculated from the data listed in **Table 1**, and are also listed in **Table 3**. Clearly, the $y_{\gamma/\text{Ni}}$ value of the treated particles (91.48/4.17) is larger than that of the untreated particles (91.74/5.63), which confirms the reduction of the Ni$_2$O$_3$ phase after the treatment, since the molar concentrations of γ-Fe$_2$O$_3$ in both untreated and treated particles can be regarded as equal.

4.3. The Mass Percentages of the Phases in the Particles

From the molar percentage of each phase, the mass percentages of the phases in both untreated and treated particles, z_i, can be deduced from

$$z_i = \frac{y_i A_i}{\sum y_i A_i} \times 100 \quad (7)$$

where y_i is the molar percentage and A_i is molecular weight of the i phase in the particles. Accordingly, the mass percentage of each phase for the two particles can

Table 3. The molar percentage of each phases in the untreated and treated particles y_i.

i	γ-Fe$_2$O$_3$	Ni$_2$O$_3$	FeCl$_3$	Fe(NO$_3$)$_3$
Untreated particles	91.74	5.63	2.63	
treated particles	91.48	4.14		4.38

be obtained from the results listed in **Table 3** and the molecular weights of γ-Fe$_2$O$_3$, Ni$_2$O$_3$, FeCl$_3$·6H$_2$O or Fe(NO$_3$)$_3$·9H$_2$O, which are listed in **Table 4**.

From the results in **Table 4**, it can be seen that the mass fractions of both γ-Fe$_2$O$_3$ and Ni$_2$O$_3$ in the treated particles are less than in the untreated particles. Therefore, the specific magnetization of the former is weaker than that of the latter, since γ-Fe$_2$O$_3$ is ferrimagnetic, Ni$_2$O$_3$ is weakly ferromagnetic [16], and both FeCl$_3$ and Fe(NO$_3$)$_3$ are paramagnetic.

4.4. The Volume Percentages of the Phases in the Particles

From the mass percentage z_i, the volume percentage of each phase in the particle system, ϕ_i, can be obtained from

$$\phi_i = \frac{z_i / \rho_i}{\sum z_i / \rho_i} \times 100 \quad (8)$$

where ϕ_i is the density of the i phase. The densities of γ-Fe$_2$O$_3$, Ni$_2$O$_3$, FeCl$_3$·6H$_2$O and Fe(NO$_3$)$_3$·9H$_2$O are 4.90, 5.32, 1.844 and 1.684g/cm^3, respectively. Thus, from the z_i values listed in **Table 4**, the values of ϕ_i can be calculated, and are listed in **Table 5**. For the treated particles, the volume of the γ-Fe$_2$O$_3$ phase should be same as for the untreated ones. The fact that the volume percentage of γ-Fe$_2$O$_3$ phase for the treated particles is less than that for the untreated particles shows that the size of the former is larger than that of the latter. This is in agreement with the TEM results.

4.5. The Density of the Particles

From both mass percentages and densities of each phase, the average density of the particles containing many phases, $<\rho>$, can be obtained from

$$\langle\rho\rangle = \frac{\sum \rho_i \phi_i}{100} = \frac{1}{\sum z_i / \rho_i} \times 100 \quad (9)$$

Using Formula (9), the average density can be estimated as 4.596 g/cm^3 and 4.102 g/cm^3 for the untreated and treated particles, respectively. For the treated particles, the density 4.102 g/cm^3 is very close to 4.125 g/cm^3, which was deduced from density measurements of the corresponding ferrofluids [12].

From the average density, the magnetization curves of

$M(=\sigma_i\rho_i)$ vs. H can be obtained from the specific magnetization, as shown in **Figure 7**. The values of saturation magnetization $M_s(=\sigma_s\cdot<\rho>)$ were obtained from σ_s as 260.09 and 168.96 kA/m for the untreated and treated particles, respectively.

5. Conclusion

Using a chemically induced transition in $FeCl_2$ solution, composite nanoparticles containing a γ-Fe_2O_3 core, Ni_2O_3 shell and $FeCl_3\cdot 6H_2O$ outermost layer, were synthesized. The $Fe(NO_3)_3$ solution treatment after synthesis dissolves $FeCl_3$ and some of the Ni_2O_3 to give a new $Fe(NO_3)_3\cdot 9H_2O$ layer on the undissolved part of the nanoparticles. This shows that during the $Fe(NO_3)_3$ treatment, it is easily absorbed on the ferrite particles to form a $Fe(NO_3)_3\cdot 9H_2O$ surface layer, a result similar to Fe_3O_4 when treated with $Fe(NO_3)_3$ [17,18]. For the composite nanoparticles with many phases, combining bulk with surface analysis using EDX, XRD and XPS reveals their structure and the molar, mass and volume percentages of each phase can be calculated. As a consequence,

Table 4. The mass percentage of each phases in the untreated and treated particles z_i.

i	γ-Fe_2O_3	Ni_2O_3	$FeCl_3\cdot 6H_2O$	$Fe(NO_3)_3\cdot 9H_2O$
Untreated particles	90.01	5.72	4.27	
Treated particles	85.62	4.01		10.73

Table 5. The percentage volume of each phases in the untreated and treated particles ϕ_i.

i	γ-Fe_2O_3	Ni_2O_3	$FeCl_3\cdot 6H_2O$	$Fe(NO_3)_3\cdot 9H_2O$
Untreated particles	84.42	4.94	10.64	
Treated particles	71.67	3.09		25.24
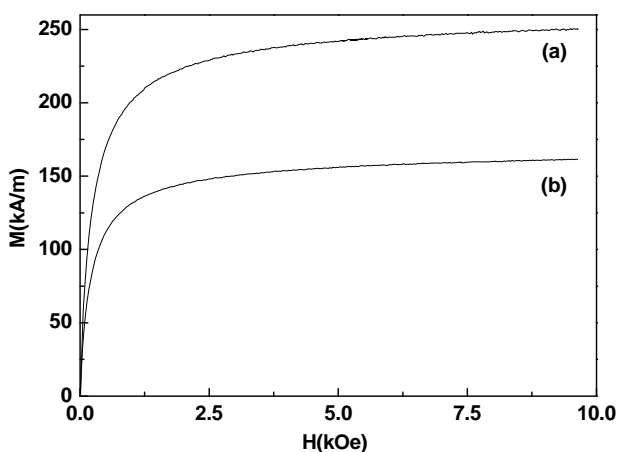
Figure 7. The magnetization curves of (a) untreated particles and (b) treated particles.

the difference of both magnetization and size between the treated and untreated particles can be explained from the phase ratios. In addition, the average density of the particles can be obtained, which is very important for the synthesis of ferrofluids with accurate volume fractions of particles. The experiments indicated that after treatment with $Fe(NO_3)_3$, although the γ-Fe_2O_3 core is unchanged, the magnetization of the treated particles becomes much weaker than that of the untreated particles. Clearly, this is evidence showing that the surfaces of magnetic nanoparticles play an important role in determining their magnetization behavior.

6. Acknowledgements

REFERENCES

[1] J. Nogués, J. Sort, V. Langlais, V. Skumryev, S. Suriñach, J. S. Muñoz, *et al.*, "Exchange Bias in Nanostructures," *Physics Reports-Review Section of Physics Letters*, Vol. 422, No. 3, 2005, pp. 65-117.

[2] M. Knobel, W. C. Nunes, L. M. Socolovsky, E. De Biasi, J. M. Vargas and J. C. Denardin, "Superparamagnetism and Other Magnetic Features in Granular Materials: A Review on Ideal and Real Systems," *Journal of Nanoscience and Nanotechnology*, Vol. 8, No. 6, 2008, pp. 2836-2857.

[3] D. V. Szabó and D. Vollath, "Nanocomposites from Coated Nanoparticles," *Advanced Materials*, Vol. 11, No. 15, 1999, pp. 1313-1316. http://dx.doi.org/10.1002/(SICI)1521-4095(199910)11:15<1313::AID-ADMA1313>3.0.CO;2-2

[4] Q. X. Liu, Z. H. Xu, J. A. Finch and R. Egerton, "A Novel Two-Step Silica-Coating Process for Engineering Magnetic Nanocomposites," *Chemistry of Materials*, Vol. 10, No. 12, 1998, pp. 3936-3940. http://dx.doi.org/10.1021/cm980370a

[5] R. E. Rosensweig, "Ferrohydrodynamic," Cambrige University, Combridge, 1985.

[6] R. Massart, "Preparation of Aqueous Magnetic Liquids in Alkaline and Acidic Media," *IEEE Transactions on Magnetics*, Vol. 17, No. 2, 1981, pp. 1247-1248. http://dx.doi.org/10.1109/TMAG.1981.1061188

[7] F. A. Tourinho, R. Franck and R. Massart, "Aqueous Ferrofluids Based on Manganese and Cobalt Ferrites," *Journal of Materials Science*, Vol. 25, No. 7, 1990, pp. 3249-3254. http://dx.doi.org/10.1007/BF00587682

[8] M. H. Sousa, F. A. Tourinho, J. Depeyrot, G. J. da Silva and M. C. F. Lara, "New Electric Double-Layered Magnetic Fluids Based on Copper, Nickel, and Zinc Ferrite Nanostructures," *The Journal of Physical Chemistry B*, Vol. 105, No. 6, 2001, pp. 1168-1175. http://dx.doi.org/10.1021/jp0039161

[9] J. Crangle, "The Magnetic Properties of Solids," Edward Arnold, London, 1977.

[10] B. Huke and M. Lücke, "Magnetic Properties of Colloidal Suspensions of Interacting Magnetic Particles," *Reports on Progress in Physics*, Vol. 67, No. 10, 2004, pp. 1731-1768. http://dx.doi.org/10.1088/0034-4885/67/10/R01

[11] Q. M. Zhang, J. Li, Y. Q. Lin, X. D. Liu and H. Miao, "The Preparation and Characterization of Ni-Fe Bioxide Composite Nanoparticles," *Journal of Alloys and Compounds*, Vol. 508, No. 2, 2010, pp. 396-399. http://dx.doi.org/10.1016/j.jallcom.2010.08.065

[12] L. H. Lin, J. Li, J. Fu, Y. Q. Lin and X. D. Liu, "Preparation, Magnetization, and Microstructure of Ionic Ferrofluids Based on Gamma-Fe_2O_3/Ni_2O_3 Composite Nanoparticles," *Materials Chemistry and Physics*, Vol. 134, No. 1, 2012, pp. 407-411. http://dx.doi.org/10.1016/j.matchemphys.2012.03.009

[13] R. Arulmurugan, G. Vaidyanathan, S. Sendhilnathan and B. Jeyadevan, "Co-Zn Ferrite Nanoparticles for Ferrofluid Preparation: Study on Magnetic Properties," *Physica B-Condensed Matter*, Vol. 363, No. 1-4, 2005, pp. 225-231. http://dx.doi.org/10.1016/j.physb.2005.03.025

[14] C. G. Granqvist and R. A. Buhrman, "Ultrafine Metal Particles," *Journal of Applied Physics*, Vol. 47, No. 5, 1976, pp. 2200-2219. http://dx.doi.org/10.1063/1.322870

[15] L. L. Chen, J. Li, Y. Q. Lin, X. D. Liu, L. H. Lin and D. C. Li, "Surface Modification and Characterization of γ-Fe_2O_3 Nanoparticles Synthesized by Chemically-Induced Transition," *Materials Chemistry and Physics*, Vol. 141, No. 2-3, 2013, pp. 828-834.

[16] Q. M. Zhang, J. Li, H. Miao and J. Fu, "Preparation of Gamma-Fe_2O_3/Ni_2O_3/$FeCl_3$($FeCl_2$) Composite Nanoparticles by Hydrothermal Process Useful for Ferrofluids," *Smart Materials Research*, Vol. 2011, 2011, Article ID: 351072. http://dx.doi.org/10.1155/2011/351072

[17] A. R. Wang, J. Li and Y. Wang, "Analysis of Fe_3O_4 Nanoparticles Treated with $Fe(NO_3)_3$," *Journal of Instrumental Analysis*, Vol. 25, No. 6, 2006, pp. 35-38. (in Chinese)

[18] J. Li, X. Y. Qiu, Y. Q. Lin, X. D. Liu, R. L. Gao and A. R. Wang, "A Study of Modified Fe_3O_4 Nanoparticles for the Synthesis of Ionic Ferrofluids," *Applied Surface Science*, Vol. 256, No. 23, 2010, pp. 6977-6981. http://dx.doi.org/10.1016/j.apsusc.2010.05.009